DOI: 10.1002/ejoc.200700455

Hemivannusal and Prevannusadials – New Sesquiterpenoids from the Marine Ciliate Protist *Euplotes vannus*: The Putative Biogenetic Precursors of Dimeric Terpenoid Vannusals

Graziano Guella,*[a] Emanuela Callone,[a] Graziano Di Giuseppe,[b] Rita Frassanito,[a] Francesco P. Frontini,[b] Ines Mancini,[a] and Fernando Dini[b]

Keywords: Terpenoids / Marine ciliates / Structure elucidation / Ab initio calculations / Endosymbionts

Hemivannusal (**6**), a bicyclic sesquiterpenoid with an unprecedented skeleton, has been isolated from the marine ciliate *Euplotes vannus* (strain TB6). The relative configuration of **6** has been established through an extended conformational search performed by molecular mechanics and refined through ab initio quantum chemical calculations. Another strain (CM1) of the same morphospecies has been found to produce the linear prevannusadial A (**7**) and the monocyclic prevannusadial B (**8**), which could represent key intermediates for the biosynthesis both of hemivannusal (**6**) and of the C30 terpenoids vannusals A and B (**5a** and **5b**), the latter pair being metabolites isolated from conspecific strains (Sil21 and BUN3) of the same *E. vannus* morphospecies. The occurrence of hemivannusal (**6**) in mass cell cultures both of an *E. vannus* endosymbiont-free strain and of a penicillin-treated *E. vannus* bacteria-infected strain strongly suggests that its biosynthesis is coded by the ciliates and not by prokaryotic endosymbiont genes. The pattern of the secondary metabolites isolated so far from different strains of *E. vannus* allows us not only to assign them a chemotaxonomic significance, but also to propose a unifying picture of their biogenesis.

Introduction

Massive cell cultures of unicellular marine ciliates of the genus *Euplotes* (Ciliophora) have been demonstrated to be a rich source of secondary metabolites (Scheme 1). In particular, the cosmopolitan morphospecies *Euplotes crassus* has yielded highly strained acetylated sesquiterpene hemiacetals (euplotane skeleton). Among them, euplotin C (**1**),[1] the structure of which has been characterized up to the absolute configuration level,[1c] has been demonstrated to be strongly bioactive, as it: 1) is able to kill, at the μM level, strains of euplotin nonproducing *Euplotes*,[1a] 2) has cytotoxic effects on free-living and parasitic protozoa, yeasts, and bacterial strains,[2] and finally 3) shows remarkable cytotoxic and apoptotic inducing action towards mouse (AtT-20) and rat (PC12) tumor cell lines.[3]

Other terpenoids with unprecedented new skeletons have also been isolated from representatives of the genus *Euplotes*. Among sesquiterpenoids, we cite here raikovenal (**2a**),[4a] isolated from *Euplotes raikovi* and built around a bicyclo[3.2.0]heptane ring system, and rarisetenolide (**3a**),[5] isolated from *Euplotes rariseta* and containing an octahydroazulene moiety. Among diterpenoids, focardin (**4**),[6] first obtained from an Antarctic strain of *Euplotes focardii*, deserves special mention since it represents a reliable taxonomic marker of the morphospecies, characterizing all pop-

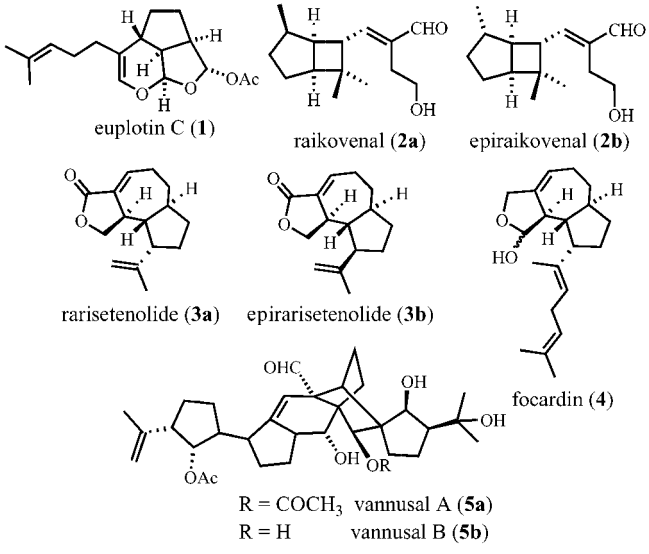

Scheme 1. Sesquiterpenoids isolated from marine ciliates of the genus *Euplotes*.

[a] Laboratorio di Chimica Bioorganica, Dipartimento di Fisica, Università di Trento,
38050 Povo-Trento, Italy
Fax: +39-461-882009
E-mail: guella@science.unitn.it
[b] Dipartimento di Biologia, Università di Pisa,
Pisa, Italy

Supporting information for this article is available on the WWW under http://www.eurjoc.org or from the author.

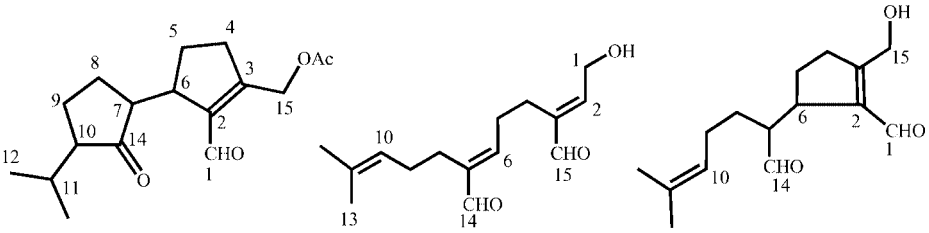

Scheme 2. Flat structure of the new sesquiterpenoids isolated from *Euplotes vannus*. Numbering follows the adopted numbering convention for farnesane.

ulations of this form, whatever their geographic origin (Antarctic or equatorial).

In contrast with the highly conservative trait in production of euplotins by all *E. crassus* populations, the occurrence of interpopulation variability in the secondary metabolites shown by the *E. raikovi* and *E. rariseta* morphospecies is mainly reflected in a chiral chemodiversity of the isolated metabolites. In fact, different populations give the epimeric skeletons epiraikovenal (**2b**)[4b] and epirariseteneolide (**3b**),[5] a finding that clearly indicates the presence of polymorphism in these morphospecies. From an evolutionary perspective, such interpopulation variation in secondary metabolites suggests the occurrence in each taxon of intramorphospecific minimal irreversible discontinuities, and hence of different evolutionary lines, even when a morphological uniformity is apparent.[7]

Recently, we have been focusing our attention on the secondary metabolites of the morphospecies *E. vannus,* which, together with *E. crassus* and *E. minuta*, constitutes a complex of evolutionarily closely related forms.[8] From a tropical population (Sil 21) of *E. vannus* two intriguing compounds with an unusual and novel C30 backbone, named vannusal A (**5a**) and vannusal B (**5b**), were isolated and it was proposed that their biogenesis arose from a deviation of the route to triterpenes.[8] However, as it will be become clear later, they might rather derive from a dimerization (possibly through aldol condensation) of a regular C15 sesquiterpenoid.

Synthetic organic chemists have also shown strong interest in ciliate terpenoids; in fact, the total synthesis of euplotin A,[9] as well as those of raikovenal and raikovenal-like metabolites,[10] have been performed. More recently, a synthetic analogue of vannusal A has also been reported.[11]

Following extensive analysis on small scale and/or massive cell cultures of other strains of *E. vannus*, we report here the isolation of new regular sesquiterpenoids from two different strains. In particular, from the strain TB6 we have isolated the new bicyclic sesquiterpenoid hemivannusal (**6**) and from the strain CM1 both the linear terpenoid prevannusadial A (**7**) and the monocyclic prevannusadial B (**8**; Scheme 2). The structures of these compounds have been elucidated by a combination of modern mass spectrometry and NMR techniques, as well as with the aid of molecular mechanics (MM) and ab initio quantum chemical (QM) calculations. Experiments aimed at establishing the biosynthetic origin of hemivannusal, which could in principle be produced from endosymbiotic bacteria, have been also performed, and the results are described here. Finally, a unifying pathway for the biosynthesis of secondary metabolites of *E. vannus* is proposed along with some suggestions concerning the mechanism by which hemivannusal might give rise to the C30 backbone metabolites.

Results and Discussion

Structure Elucidation of Hemivannusal

Mass spectrometry (EI-MS and EI-HRMS, LC-ESI-MS/MS) furnished a molecular composition of $C_{17}H_{24}O_4$ for hemivannusal, implying six degrees of unsaturation. Since NMR and IR spectra revealed the presence of one tetrasubstituted carbon–carbon double bond and three carbonyl groups, the molecule must be bicyclic. ^1H and ^{13}C NMR spectroscopy also revealed the presence of one acetyl group [δ_H = 2.11 ppm (s) in $CDCl_3$ and δ_H = 1.59 ppm (s) in C_6D_6; δ_C = 20.74 ppm (q)], one α-β-unsaturated aldehyde singlet proton (δ_H = 10.07 ppm; δ_C = 187.77 ppm), a methylene group deshielded by an ester group [δ_H = 5.05 ppm, AB system; δ_C = 59.68 ppm (t)], a strongly deshielded methine proton belonging to a nonheterosubstituted secondary carbon atom [δ_H = 3.71 ppm (m); δ_C = 43.12 ppm (d)] and an isopropyl group side chain showing diasteroisotopic methyl groups [δ_H = 0.78 (d) and 0.96 ppm (d); δ_C = 18.35 (q) and 20.66 ppm (q), respectively]. Carbon connectivities were mainly established by COSY and differential homonuclear decoupling experiments. In particular, the long-range couplings of aldehyde proton with methine 6-H and of 15-H_2 with the allylic methylene protons at C-4 allowed us to establish the regiochemical position of the substituents on the C2=C3 bond. A combination of 1D differential proton decoupling (DDDS, COSY, HMBC, and HMQC-NMR) experiments supported the connection of these fragments as shown in **6** (Scheme 2).

The Relative Stereochemistry

In order to establish the relative configurations in **6**, in particular at C6–C7, we must correlate the stereochemistry of the chiral centers on the two rings. Since they are linked

Table 1. NMR spectroscopic data for hemivannusal (**6**) in $CDCl_3$ at 298 K (^1H at 400 MHz, ^{13}C at 100 MHz).

C-Atom	δ_H [ppm], *J* [Hz]	δ_C [ppm]	nOe enhancement at
1	10.07 s	187.8d	15-H_2
2	–	116.3 s	
3	–	not detected	
4	α 2.56 br ddd(5.1, 9.6,15.5) β 2.62 br ddd(6.8, 6.8, 15.5)	35.4 t	15-H_2, 5-H_2
5	α 2.06 ddd (6.8, 9.6, 13.8)	24.1 t	6-H, 5β-H, 15α-H
	β 1.37 dddd (5.1, 6.0, 6.8, 13.8)		15-βH, 5α-H
6	3.71 ddd (3.9, 6.0, 9.6)	43.1 d	7-H, 5α-H
7	α 2.81 ddd (3.9, 8.3, 12.4)	52.9 d	6-H, 8α-H, 8β-H, 9α-H, Me-13
8	α 1.75 ddd (6.4, 8.3, 12.2)	24.1 t	7-H, 9α-H, 8β-H
	β 1.34 dddd (6.4, 12.4, 12.4, 3.8)		8α-H, 9β-H
9	α 1.52 dddd (6.4, 11.2, 12.4,13.8)	21.9 t	7-H, 9β-H, 10-H, Me-13
	β 1.96 ddd (6.4, 8.5, 13.8)		9α-H, 8β-H, Me-12
10	β 1.92 ddd (4.4, 8.5, 11.2)	56.4 d	9β-H, Me-12
11	2.14 dseptet (4.4, 6.9)	27.6 d	10-H, Me-12, Me-13
12	0.96 d (6.9)	20.7 q	11-H, 10-H, 9β-H
13	0.78 d (6.9)	18.4 q	11-H, 9α-H
14	–	207.5 s	
15	5.03, 5.07 AB system (14.3)	59.7 t	4α-H, 4β-H
*CH_3*CO-	2.11 s	20.7 q	–
CH_3*CO*-	–	170.4	–

by carbon–carbon single bonds around which free rotation would be expected to occur, the problem is far from being an obvious matter. In particular, whereas the *trans* stereochemistry between 7-H and 10-H can be established from the absence of any nOe effect between them either in 1D- or in 2D-NOESY experiments, the 3D-relationship of such configurations to the C-6 stereogenic center cannot, in general, be inferred from vicinal couplings or NOE effects between 7-H and 6-H, since they represent thermal averaged values of different C6–C7 rotamers.

Assuming an α position for 7-H (*S**, in the enantiomeric form shown here), the configuration at C-10 can be unambiguously assigned as *S**, thus leaving 10-H in a pseudoaxial β position, on the grounds both of the above-mentioned absence of any nOe effect between 7-H and 10-H and, more importantly, of the observed coupling patterns of all the protons on the embedding ring. A careful coupling pattern analysis of these protons (obtained by 1D-NMR differential decoupling experiments) provided the *J* scalar coupling values and nOe effects reported in Table 1, which are nicely in agreement with those expected for a *trans* 1,3-disubstituted cyclopentanone ring. In particular, the mutual dipolar couplings of 7-H with 6-H, of 8α-H with 9α-H, of 6-H with 5α-H, of Me-12 with 10-H and 11-H, and of Me-13 with 9α-H, 10-H, and 7-H (weak but detectable in differential 1D-nOe measurements), helped us to assign all the protons in the NMR spectrum of **6** and indicated a preferred conformation among the C10–C11 rotamers. Indeed, in order to avoid *gauche* repulsive interaction due to 1,3-allylic strain with the carbonyl group,[12] the C10–C11 bond adopts a conformation in which the shielded Me-13 (δ_H = 0.79 ppm) keeps to a plane orthogonal to the mean plane of the ring, thus showing dipolar relaxation with α protons 7-H and 9α-H, while Me-12 lies on the mean plane of the same ring, thus showing nOe effects with 10-H and 9β-H. The relevant contribution of such a conformation is supported by the low value of $^3J_{10,11}$, of 4.8 Hz. Since rotation around C10–C11 would be expected to be very fast on the NMR timescale, the outcome of the nOe effects and the coupling value indicates a largely preferred *gauche* rotamer with a H10–C10–C11–H11 torsion angle of about –60° for a (6*R**,7*S**,10*S**) stereochemistry.

Results from Molecular Mechanics and Quantum Chemical Calculations

In order to arrive at the complete relative stereochemistry of **6**, we decided to undertake a full conformational search with the aid of the GMMX program,[13] considering the two alternative configurations epimeric at C-6 but with fixed *trans* relative stereochemistry at C-7 and C-10: that is, (6*S**,7*S**,10*S**) and (6*R**,7*S**,10*S**). Conformational searching was carried out, allowing both ring-flipping and single-bond rotations through the use of the default values of the program; however, the analysis was restricted to bond rotations only around C6–C7 and C10–C11 bonds.

Calculations were in fact performed on a simplified model of **6** in which the acetyl function had been removed, thus leaving C-15 as a methyl group. This model would be expected to preserve all the structural features affecting the overall conformational freedom of hemivannusal (**6**); it was chosen not only to decrease the calculation times but mainly to avoid the subtle, and possibly unreliable, small differences in strain energy deriving from the C3–C15 and C15–OAc conformational degrees of freedom. Finally, only the *transoid* conformation of the aldehyde group at C-1 (O=C1–C2–C3 torsional angle at 180°) was considered in the full conformational search, since in the 1D-detected dipolar couplings the aldehyde proton showed strong spatial interaction only with H_2–C15. Moreover, a preliminary conformational search aimed at establishing the relative stability between *syn*/*anti* C1–C2 rotamers performed both on **6** and on its deacetylated model suggested a strong prefer-

ence (more than 2.0 kcal mol^{-1}) for the *transoid* rotamer with respect to its *cisoid* counterpart. With this model and within these constraints, the main outcome of MM calculations was the significant conformational control exerted by the C-6 configuration on the mutual spatial orientation of the rings. In fact, for the (6*S**,7*S**,10*S**) diastereoisomer we found a clear dominance of a family of stable "folded" conformations with the two rings in a quasiorthogonal spatial disposition, thus implying a preferential *gauche* relationship between 6-H and 7-H (g^-_{6-7} rotamer, conformation on the left in Scheme 3). On the other hand, in the (6*S**,7*R**,10*R**) epimer no such conformational preference seems to operate, as similar strain energies were calculated for the three g^-_{6-7}, *anti* $_{6-7}$ and g^+_{6-7} rotamers.

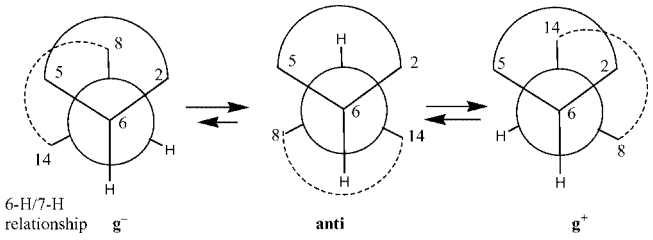

Scheme 3. Stable rotamers around the C6–C7 single bond of the model compound **6M** as obtained from MM and ab initio quantum chemical calculations.

Unfortunately, MM calculations carried out on the same (6*S**,7*S**,10*S**) hemivannusal model were not in good agreement with experimental observations in the evaluation of the relative stabilities of C10–C11 rotamers. In fact, even though the family of the g^-_{6-7} rotamers were found to be significantly more stable (>2 kcal mol^{-1}) than the families of the *anti*$_{6-7}$ and g^+_{6-7} rotamers, the $g^-_{6-7}g^-_{10,11}$ was calculated to be more stable than the corresponding g^-_{6-7}*anti*$_{10,11}$ and $g^-_{6-7}g^+_{10,11}$ conformations by only 0.13 and 0.42 kcal mol^{-1}, respectively. Thus, the differences in the MM3 strain energies are not so high as to explain the experimentally observed Boltzmann-averaged $J_{10,11}$ vicinal coupling, since at 298 K the C10–C11 rotamers g$^-$/*anti*/g+ ratio is evaluated to be 44:36:20. It must be underlined that such an energy profile would also lead to a strong disagreement with the experimentally observed nOe effects of the methyl groups Me-12 and Me-13. As clearly shown in the NOESY spectrum of **6** (Figure 1), besides the common trivial nOe effect with 11-H, the two Me groups are involved in exclusive dipolar couplings, a possibility that cannot be accounted for on the basis of the MM3-evaluated conformational populations around the C10–C11 single bond.

Due to the fast rotation around the C10–C11 bond, under such equilibrium conditions the Me groups would have almost the same chemical neighbor and would show almost identical dipolar couplings, neither of which expectations were actually observed.

We were well aware that small errors in the calculated values of strain energies could result in large differences in conformer populations and, consequently, in calculated

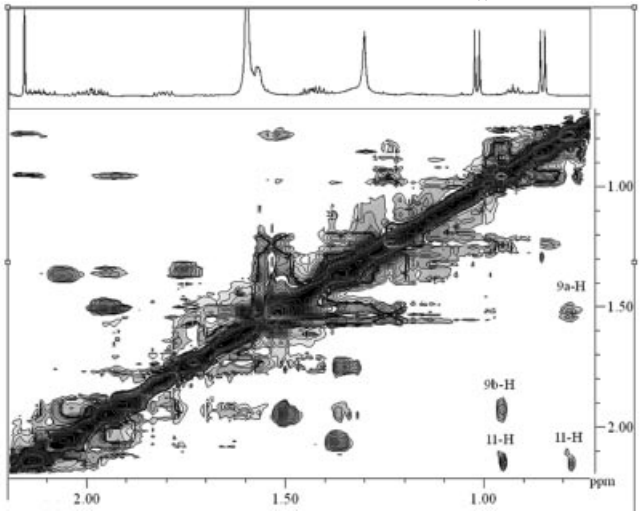

Figure 1. NOESY spectrum (high-field region) of hemivannusal (**6**) at 298 K in $CDCl_3$.

NMR parameters. We therefore turned our attention to the more reliable (and demanding) ab initio quantum chemical calculations on the same simplified model of **6** (lacking the acetyl function and with the –CHO group in the minimized *s-trans* conformation) on which the MM conformational search had been carried out. The MM-minimized rotamers were used as initial input structures, and the geometry was optimized at the Hartree–Fock 3–21G level of theory and finally energy-minimized at higher level by using DFT/B3LYP 6–311G+(d,p) as implemented in the Gaussian03 suite of programs.[14] We soon realized that the DFT-calculated energy profile of stable conformers for the (6*S**,7*S**,10*S**) epimer, although in qualitative agreement with the MM results, was significantly changed. In fact, even though the g^-_{6-7} family was again found to be largely prevalent over the *anti*$_{6-7}$ and the g^+_{6-7} families, the population ratio among the 10H–11H rotamers was found here to be = 86:8:6, thus providing a clear-cut explanation of the Me-12 and Me-13 dipolar couplings. The DFT/B3LYP calculations thus showed that the g^-g^- structure (Figure 2) should play a dominant role.

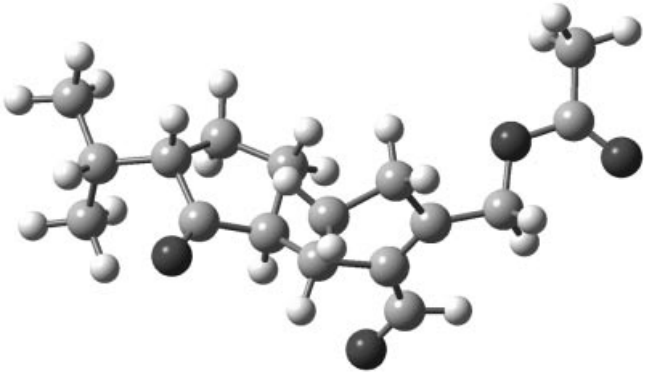

Figure 2. 3D-structure (relative stereochemistry) of hemivannusal (**6**) as inferred from NMR spectroscopic data and quantum chemical calculations.

In the same way, the DFT/B3LYP-calculated energy profile for the (6*R**,7*S**,10*S**) epimer was found to be quite similar in its general outcome to that obtained by MM3 calculations. In fact, even by the ab initio quantum chemical approach, no such strong conformational control is expected for this epimer. On these grounds, we can suggest that the relative configuration of hemivannusal (**6**) is (6*S**,7*S**,10*S**).

Structure Elucidation of Prevannusadials

The main metabolite, prevannusadial A (**7**), isolated from strain CM1 has a molecular formula $C_{15}H_{22}O_3$ as established by HRMS (Experimental Section) measurements, suggesting five degrees of unsaturation. Since deshielded signals in its ^{1}H NMR spectrum are attributable to two aldehyde protons and to three olefinic protons in trisubstituted C=C systems, the molecule must be acyclic. The last oxygen atom implicit in the molecular formula was easily recognized by NMR and IR spectra as belonging to a primary alcohol function. Extensive differential decoupling experiments together with COSY allowed us firmly to establish the positions C-14 and C-15 for the aldehyde groups and the C-1 for the primary –OH function. Moreover, the characteristic δ_H values for the α,β-unsaturated aldehyde proton at δ = 9.34 and 9.44 ppm, the values of some relevant ^{13}C resonances (strong γ-*gauche* shielding effects observed for all the allylic carbons), and the results of nOe experiments using difference spectroscopy techniques (strong effects measured on 2-H and 6-H upon irradiation on the aldehyde protons 15-H and 14-H, respectively) were used for assigning *E* stereochemistry at the double bonds in **7**, which thus represents an unprecedented oxidized form of (*Z*,*Z*)-farnesol. During NMR measurements, carried out in $CDCl_3$, **7** was seen to convert slowly into the hemiacetal **10** deriving from nucleophilic attack of the hydroxy group at C-1 on the carbonyl group at C-15, possibly through **9**, the 2,3*Z* stereoisomer of **7** (see Scheme 4, discussed below). Actually, structure **10** was only inferred from ^{1}H NMR spectroscopic measurements on a sample in which its relative amount was quite low (about 20% of **7**). The presence of the hemiacetal moiety finds strong support in the detection in the downfield region of the ^{1}H NMR spectrum of: 1) vicinal diastereotopic protons at C-1 (δ_H = 4.53 and 4.69 ppm) as a broad AB system, 2) 15-H at δ_H = 5.65 ppm as doublet, and 3) 2-H as a multiplet at δ_H = 5.81 ppm. On the other hand, the δ_H value of 9.36 ppm (s) for the aldehyde proton 14-H indicates *E* stereochemistry at the C6=C7 bond.

The minor metabolite from the CM1 strain, prevannusadial B (**8**), was isolated in very low amounts and its structure was established by direct comparison of its ^{1}H NMR spectrum with those reported in the literature either for the "diterpenoid 9"[15] isolated by Paul and Fenical from a Caribbean *Udotea* species (*U. flabellum*) or for petiodial, isolated by Fattorusso et al.[16] from a Mediterranean *Udotea* species (*U. petiolata*). Characteristic aldehyde protons at δ_H = 10.14 (s) and 9.63 ppm (d; 2.1 Hz), deshielded protons at C-1 as a br. s at δ_H = 4.63 ppm and mutually coupled multiplet signals at δ_H = 3.42 and 2.80 ppm, assigned to 6-H and 7-H, respectively, perfectly matched the reported data for these protons in the above-mentioned terpenoids, even if, due to scarcity of material, the relative configurations at the C-6 and C-7 chiral centers could not be established. Prevannusadial B (**8**), therefore, represents the deprenyl analogue of these *Udotea* diterpenoids; a situation that

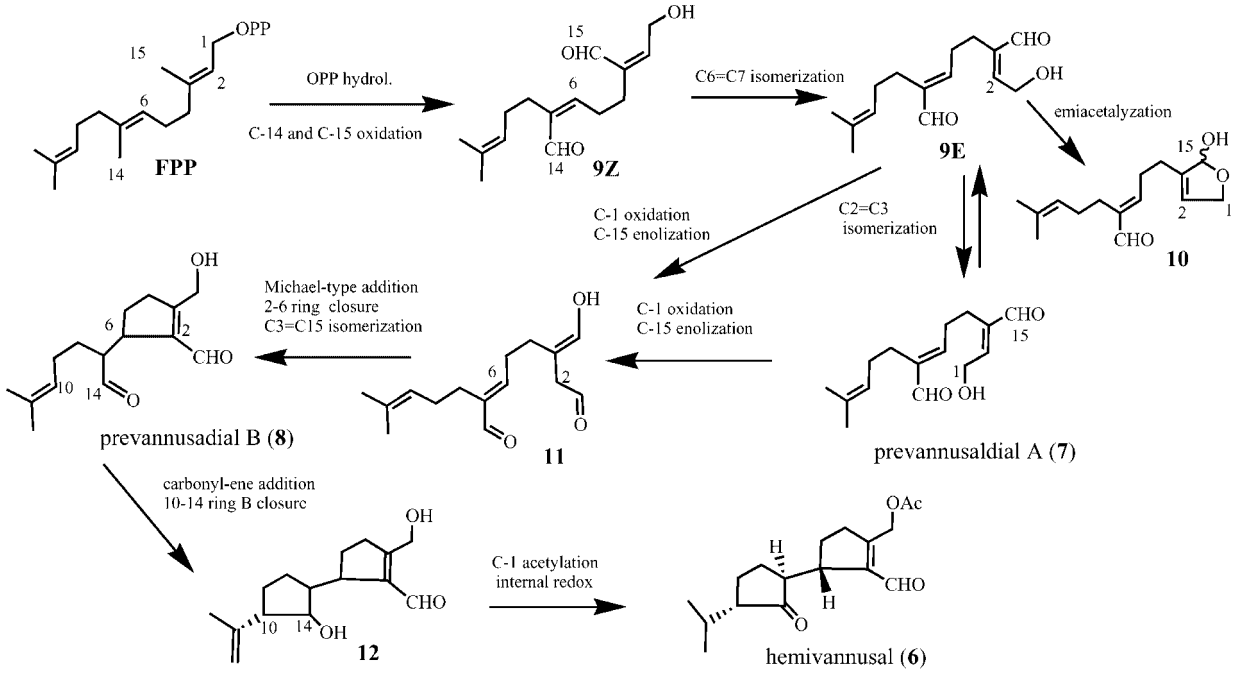

Scheme 4. Proposed biogenetic scheme for the biosynthesis of some sesquiterpenoids isolated from marine ciliates of the genus *Euplotes*.

strongly resembles circumstances we have already observed between the linear sesquiterpenoid preuplotin isolated from many different strains of *E. crassus*[1b] and the linear udoteal diterpenoids isolated from the tropical green alga *U. flabellum*.[17]

Is Hemivannusal a True Ciliate Metabolite?

It is often reported that secondary metabolite production might be mediated by prokaryotic (bacteria) endosymbionts harbored by eukaryotic microorganisms. As a matter of fact, ciliate cells represent a suitable econiche for endosymbiotic colonizers, mainly of prokaryotic nature, and specific bacterial endosymbionts characterize several *Euplotes* taxa and are known to infect all the members of the comprised populations. In such cases, treatment with antibiotic drugs (penicillins) has demonstrated that peculiar features are bestowed on eukaryotic guests by the prokaryotic hosts. In most of the *Euplotes* taxa, the prokaryotic infection is far more flexible: inter- and intrapopulation variability occurs when either the presence/absence or the level of the host infection are involved. *E. vannus* intrapopulation variability allowed us to isolate both the significantly infected strain TB6 and the endosymbiont-free strain Male5. According to our phylogenetic analysis based on 18S rDNA, ITS1 and ITS2 (nuclear), and 16S rDNA (mitochondrial) gene sequences, Male5 has been demonstrated to be genetically identical to the TB6 strain. HPLC-MS analysis of an organic extract obtained from a small-scale cell culture of this *E. vannus* strain (Male5) clearly indicated the presence of the same major secondary metabolite (hemivannusal, **6**) in almost the same amount as produced by the *E. vannus* TB6 strain. This result strongly suggests that **6** (and reasonably all the metabolites so far isolated from marine *Euplotes*) is a "true ciliate metabolite" rather than a product of the harbored prokaryotic endosymbionts. As further support for this conclusion, we must underline that when mass cultures of the strains TB6 and CM1 were treated with antibiotics (penicillin G 600 U mL^{-1}) for eight days to prevent bacterial multiplication, no significant variation in secondary metabolite production between the penicillin-treated and untreated mass cultures occurred, regardless of the food used (microalgae or bacteria) to cause them to thrive. At each fission of a ciliate cell, the bacterial endosymbiotic population was halved in the two ciliate fission descendants, whilst the effect of such treatment was not to stop but only to decrease the fission rates of ciliates to 1.0–1.3 fissions per day. At the end of treatment, thin sections of at least 20 cells for every strain were subjected to transmission electron microscopy. The intracellular concentrations of the symbiotic population had decreased from 10–30 bacteria for the untreated ciliate cells to 0–3 bacteria for the penicillin-treated descendants.

Biogenetic Considerations

The biosynthesis of hemivannusal (**6**) from a farnesyl pyrophosphate (FPP) may be imagined (Scheme 4), which implies prevannusadial A (**7**) as a putative precursor. In our view, after C-1 pyrophosphate hydrolysis, oxidation at the C-14 and C-15 methyl groups should afford the putative intermediate **9*Z*** bearing two α,β-unsaturated aldehyde functions with *Z* stereochemistry. Following *Z*→*E* isomerization of the 6,7 double bond, the intermediate **9*E*** could then lead to: 1) prevannusadial A (**7**), after *Z*→*E* isomerization of 2,3 double bond, 2) the unsaturated γ-lactol **10**, after intramolecular nucleophilic addition of the C-1 hydroxy group to the C-15 aldehyde function, and 3) the intermediate **11** after oxidation of the allylic hydroxy group of **7** and enolization of the C-15 formyl group.

The intermediate **11** could in turn be converted in a Michael-type intramolecular addition of the nucleophilic

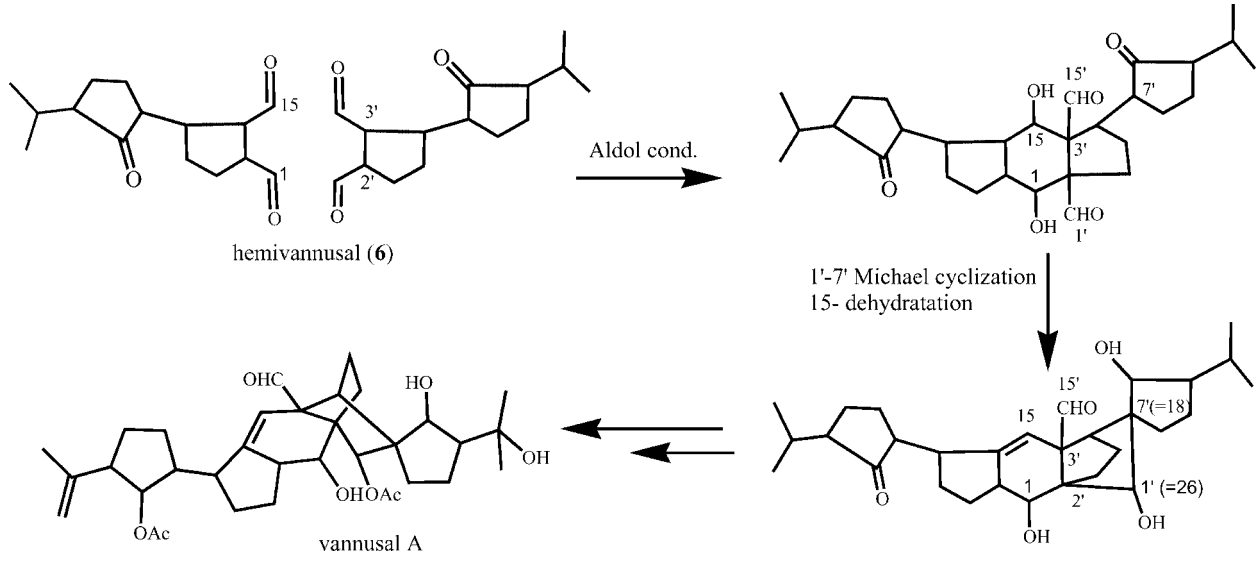

Scheme 5. Proposed biosynthetic route toward the C30 backbone metabolite vannusal B (**5b**) from suitable sesquiterpenoids with hemivannusane skeleton.

center C-2 (activated by the C-1 carbonyl group) to the electrophilic C-6 center, leading to prevannusadial B (**8**) and, through an intramolecular [C14–C10] carbonyl-ene process, to the bicyclic hypothetical intermediate **12**. The main TB6 metabolite, hemivannusal (**6**), could finally be obtained after acetylation of the free primary –OH group (an effective protection against formation of **10**-like lactol derivatives) and internal redox reaction taking place in the isopropenyl cyclopentanol moiety, a process with ample precedents in literature reports on carbonyl-ene synthetic procedures.[18]

Further support for our viewpoint is provided by the occurrence of the "C30 irregular triterpenoids" vannusal A (**5a**) and vannusal B (**5b**) from tropical strains of the same *E. vannus* morphospecies.[8] These were believed[8] to arise from a deviating route of the squalene pathway to triterpenes, but their biosynthesis is now better explained in terms of an ultimate nucleophilic dimerization of two molecules possessing the hemivannusane regular sesquiterpenoid skeleton as shown in Scheme 5. In particular, C30 terpenoids **5a** and **5b**[8] should derive from a (concerted?) condensation of the "peripheral" C-1 and C-15 electron-poor carbonyl groups of the first hemivannusane moiety with the "internal" C-2′ and C-3′ electron-rich centers of the second moiety. In our biomimetic proposal, the [C1–C7] cyclization should be followed by simple functional transformations (water elimination and addition) leading to the intricate ring systems of vannusals A (**5a**) and B (**5b**).

Conclusions

A bicyclic sesquiterpenoid, hemivannusal (**6**), with an unprecedented skeleton has been isolated from a massive cell culture of the marine ciliate *E. vannus* (strain TB6). Its structure has been elucidated by combining conventional experimental approaches based on NMR spectroscopic data with molecular mechanics and quantum chemical calculations performed at high levels of theory on a suitable 3D model of hemivannusal itself. We also reported the structural characterization of the linear prevannusadial A (**7**) and of the monocyclic prevannusadial B (**8**), sesquiterpenoids bearing aldehyde groups at the relevant C-14 and C-15 positions of the farnesane chain, both isolated from a different strain (CM1) of the same *E. vannus* morphospecies. This finding allows us to propose here for the first time a unifying picture of the biogenesis of secondary metabolites so far isolated from marine ciliates belonging to *E. vannus* morphospecies.

Another outcome of the work presented here is that the "secondary metabolites diversity" among morphospecies belonging to the *E. crassus*/*E. vannus*/*E. minuta* complex can be explained on the grounds of metabolic divergence in the last part of the "methyl oxidation + nucleophilic additions" pathway. Indeed, whereas *E. vannus* precursor metabolites **7** and **8** can afford hemivannusal (**6**) through a 10,14 carbonyl-ene-type reaction, the putative precursor metabolite of *E. crassus* [preuplotin, bis(enol acetate) analogue of **11**] should afford the tricyclic ring system of euplotin C (and even of euplotins A–B) through a cascade of intramolecular acetalization processes.[1]

Since hemivannusal (**6**) is also present in cell cultures of an endosymbiont-free strain of the same morphospecies (genetically identical to the TB6 infected strain) and in penicillin-treated cell cultures of the TB6 strain itself, their xenobiotic origin from bacteria, living as symbionts in ciliate cells, can reasonably be ruled out.

Experimental Section

General Methods: Proton NMR spectra (^{1}H NMR, COSY, NOESY) for **6** were recorded with a Bruker-Avance 400 MHz NMR spectrometer, whereas ^{1}H NMR spectra for **7**, **8**, and derivative **9**, as well as ^{13}C NMR, DQCOSY, APT, and HMQC spectra for all the described compounds, were recorded with a Varian XL 300 MHz instrument in $CDCl_3$. LC/ESI-MS analysis was performed on a reverse-phase column (Agilent Zorbax eclipse XDB-C18 4.6 × 150 mm × 3.5 μm) with CH_3CN/H_2O (Riedel de Haën) 7:3, 0.9 mL min^{-1}, split UV/MS 7/3, λ 250 nm, 5 μL injected, mounted on a Hewlett–Packard HP1100 HPLC-UV Diode Array system combined with an Esquire LC 0.98 Bruker–Daltonics ion trap mass spectrometer. MS conditions: source temp. 300 °C, nebulizing gas N_2, 4 L min^{-1}, positive ion mode, ISV 4 kV, OV 38.3 V, scan range 100–1000 *m*/*z*. EI-HRMS was performed with a Kratos-MS80 magnetic mass spectrometer, mode EI-70eV, Solid Probe, probe temp. 115°. Polarimetric data were obtained with a Jasco–DIP–181 apparatus, reporting $[\alpha]_D$ in dm^{-1} deg mL g^{-1}. CD data were obtained with a Jasco–J–710 spectropolarimeter, and give as $\Delta\varepsilon$ (λ) (λ_{max} in nm, ε in mol^{-1} dm^3 cm^{-1}). FTIR experiments were performed with a Bio-Rad FTS 185 spectrometer in ATR configuration equipped with a DTGS detector with CsI window, KBr beamsplitter, and ATR attachment by Specac. The instrument was purged with constant dry air flux; absorption region $\Delta\tilde{\nu}$ 4000–1000 cm^{-1}; a clean ATR crystal was used as background. Spectra processing was carried out with the aid of the Bio-Rad Win-IR software package. Molecular mechanics calculations were carried out with the aid of the computer program GMMX as implemented in PCMODEL 7.0.[13] All the minimized structures falling in a strain-energy window of 3.0 kcal mol^{-1} were saved and finally minimized with both MMX and MM3 force fields, keeping only those falling in a 2.0 kcal mol^{-1}. Ab initio calculations were performed with the Gaussian 03 program suite[14] utilizing unrestricted hybrid density functional molecular orbital theory with a Lee–Yang–Parr correlation functional[18] a Becke 3-parameter exchange functional (B3LYP, for example),[19] and basis sets of 6–311+G(d,p).[20]

Ciliate Strain Collection, Culturing and Isolation of the Metabolites

Euplotes vannus is a cosmopolitan morphospecies. Its analyzed strains were representative of populations of different geographical origin: CM1 from Cap Martin (France), TB6 from Tanabe (Japan), and Male5 from Pula (Italy). Interpopulation variation in genetic determinants following geographical separation would be expected to occur, and would result in the production of distinctive secondary metabolic products. Strains were established starting from single naturally occurring cells to obtain cellular line clones. The *E. vannus* strains feed on both microalgae and bacteria. The marine microalgae *Dunaliella salina* was used as the exclusive food organism for growing the analytical mass cultures, since the span between two successive cellular fissions of *E. vannus* proved to be shorter than with bacterial diets, indicating higher metabolic and genetic capabilities of ciliate for maximizing materials and energy gains

from the engulfed microalgal prey. Mass cultures were grown in defined salt water (32‰), sterilized by autoclaving, and inoculated with the microalgae. This last had previously been incubated at 23 ± 1 °C in a 12 h light/dark regimen for at least ten days inside a daylight (Osram Daylight lamp, 36 W/10) and fluorescent lamp (Osram Fluora lamp, 40 W/77) illuminated incubator system before use. Starved cells from mass cultures of the strain TB6 were pelletted by successive centrifugation rounds to provide 6.2 mL of closely packed ciliates (ca. 2.49×10^8). In each round, pelletted cells were suspended in ethanol, filtered, and finally washed. The total ethanol extract was evaporated and then partitioned between hexane/ethyl acetate 8:2 and water. The organic extract was initially purified by flash chromatography (RP-18 LiChroCART250–4 5 μm Merck, acetonitrile/methanol gradient elution). The metabolite of interest, contained in the first fraction, was further purified by HPLC (Si-60 Merck LiChrosphere column, *n*-hexane/*i*PrOH 95:5, 5 mL min^{-1}), giving pure **6** (t_R = 7.6 min, 1.5 mg).

The collecting, culturing, and pelletting procedures involving the strain CM1 mimicked those for the strain TB6. The total ethanol extract obtained from 3.9 mL of pelletted ciliates (ca. 1.6×10^8) was evaporated and then partitioned between *n*-hexane/ethyl acetate 8:2 and water. The crude organic extract (180 mg) was initially purified by flash chromatography (CN, *n*-hexane/ethyl acetate gradient elution). The metabolites of interest, contained in the 3rd and 4th fractions, were further purified by HPLC (RP-18 Merck LiChrosphere column, CH_3CN/H_2O 1:1, 6 mL min^{-1}), giving pure **7** (t_R = 8.2 min, ca. 0.5 mg) and **8** (t_R = 9 min, ca. 0.5 mg).

The ethanol extract obtained from 0.2 mL of pelletted Male5 cells (ca. 1×10^7) was directly injected (5 μL) into the HPLC column and MS-analyzed as described in the "General Methods" section. The occurrence of hemivannusal was confirmed by the observation of the same retention time (t_R 3.8 min), UV spectrum (λ_{max} 250 nm in CH_3CN/H_2O 8:2), and ESI(+) MS spectrum ($[M + Na]^+$ pseudomolecular ion at *m*/*z* 315) as those of pure **6** used as reference. A comparison with the UV integrated area of the hemivannusal peak as obtained from an identical injected volume (5 μL) of TB6 and Male5 ethanol extracts derived from a similar cell number suggests that the two strains produce **6** in a similar overall yield.

(6*S,7*S**,10*S**)-Hemivannusal (6):** Colorless oil. NMR spectroscopic data (see Table 1). CD (EtOH): λ_{max} ($\Delta\varepsilon$) = 229 (+3.1), 256 (–1.0), 303 (+ 2.0) nm. FTIR (neat): $\tilde{\nu}$ = 1730 (very strong), 1669 (strong) cm^{-1}. UV (EtOH): λ_{max} (ε, mol^{-1} dm^3 cm^{-1}) = 249 (9600) nm. MS (70 eV, EI): *m*/*z* (%) = 292 (1) $[M]^{+\cdot}$, 250 (1) $[M - CH_2{=}CO]^{+\cdot}$, 232 (42) $[M - CH_3COOH]^{+\cdot}$, 214 (16) $[M - CH_3COOH - CO]^{+\cdot}$, 189 (11) $[M - CH_3COOH - CO - CH(CH_3)_2]^+$, 171 (12), 161 (17), 124 (24), 107 (100), 43 (78). MS (ESI+): *m*/*z* = 315 $[M + Na]^+$. HRMS (EI): calcd. for $C_{15}H_{20}O_2$ 232.1463; found 232.1458 ± 0.0020.

Prevannusadial A (7): Colorless oil. ^{1}H NMR (300 MHz, $CDCl_3$): δ = 9.44 (s, 1 H, 15-H), 9.34 (s, 1 H, 14-H), 6.63 (t, *J* = 6.0 Hz, 1 H, 2-H), 6.38 (t, *J* = 6.0 Hz, 1 H, 6-H), 5.06 (br. t, *J* = 6.7 Hz, 1 H, 10-H), 4.56, 4.53 (AB system, J_{AB} = 12.2 Hz, 2 H, 1-H_2), 2.44 (m, 4 H, 4-H_2 and 5-H_2), 2.22 (m, 2 H, 8-H_2), 2.02 (m, 2 H, 9-H_2), 1.67 (br. s, 3 H, 12-H_3), 1.58 (br. s, 3 H, 13-H_3) ppm. NOE 1D observed on 2-H and on 6-H resonances on irradiation at δ = 9.44 and 9.34 ppm, respectively. ^{13}C NMR (100 MHz, $CDCl_3$): δ = 194.97 (d, C-15), 194.13 (d, C-14), 152.77 (d, C-2), 152.22 (d, C-6), 135.68 (s, C-11), 123.28 (d, C-10), 59.46 (t, C-1), 27.66 (t), 27.02 (t) 25.68 (q, C12), 24.18 (t), 23.41 (t), 17.65 (q, C-13) ppm. UV (EtOH): λ_{max} (ε, mol^{-1} dm^3 cm^{-1}) = 251 (5600) nm. MS (70 eV, EI): *m*/*z* (%) = 232 (3) $[M - H_2O]^{+\cdot}$, 217 (2) $[M - H_2O - Me]^+$, 203 (4) $[M - H_2O - CHO]^+$, 163 (4) $[M - H_2O - C_5H_9]^+$, 69 (100). HRMS (EI): calcd. for $C_{15}H_{20}O_2$ 232.1463; found 232.1465 ± 0.0020.

Prevannusadial B (8): Colorless oil. ^{1}H NMR (300 MHz, $CDCl_3$): δ = 10.14 (s, 1 H, 1-H), 9.63 (d, *J* = 2.1 Hz, 1 H, 14-H), 3.42 (m, 1 H, 6-H), 5.06 (m, 3 H, 12-H_2 and 10-H), 2.80 (m, 1 H, 7-H), 2.61 (m, 2 H, 4-H_2), 1.67 (br. s, 3 H, 12-H_3), 1.58 (br. s 3 H, 13-H_3) ppm. UV (EtOH); λ_{max} (ε, mol^{-1} dm^3 cm^{-1}) = 251 (5100) nm. MS (70 eV, EI): *m*/*z* (%) = 232 (2) $[M - H_2O]^{+\cdot}$, 203 (4) $[M - H_2O - CHO]^+$, 163 (4) $[M - H_2O - C_5H_9]^+$, 69 (100). HRMS (EI): calcd. for $C_{15}H_{20}O_2$ 232.1463; found 232.1458 ± 0.0020.

Supporting Information (see footnote on the first page of this article): ^{1}H NMR, COSY, and NOESY spectra of hemivannusal (**6**) and color representation of hemivannusal (**6**) as obtained from MM and ab initio calculations.

Acknowledgments

This research was developed within the framework of the project INTERREG III A Italy-France (Sardegna-Corsica-Toscana) and financially supported by the Province of Livorno (Italy). Additional support was provided by funds of the Department of Physics, University of Trento and of the Department of Biology, University of Pisa. The authors thank Adriano Sterni for MS measurements.

[1] a) F. Dini, G. Guella, P. Giubbilini, I. Mancini, F. Pietra, *Naturwissenschaften* **1993**, *80*, 84–86; b) G. Guella, F. Dini, A. Tomei, F. Pietra, *J. Chem. Soc. Perkin Trans. 1* **1994**, *2*, 161–166; c) G. Guella, F. Dini, F. Pietra, *Helv. Chim. Acta* **1996**, *79*, 710–717; d) G. Guella, F. Dini, F. Pietra, *Helv. Chim. Acta* **1996**, *79*, 710–717.

[2] D. Savoia, C. Avanzini, T. Allice, E. Callone, G. Guella, F. Dini, *Antimicrob. Agents Chemoth.* **2004**, *48*, 3828–3833.

[3] a) D. Cervia, D. Martini, M. Garcia-Gil, G. Di Giuseppe, G. Guella, F. Dini, P. Bagnoli, *Apoptosis* **2006**, *11*, 829–843; b) D. Cervia, M. Garcia-Gil, E. Simonetti, G. Di Giuseppe, G. Guella, P. Bagnoli, F. Dini, *Apoptosis*, **2007**, accepted.

[4] a) G. Guella, F. Dini, F. Erra, F. Pietra, *J. Chem. Soc. Chem. Commun.* **1994**, *22*, 2585–2586; b) G. Guella, F. Dini, F. Pietra, *Helv. Chim. Acta* **1995**, *78*, 1747–1754.

[5] G. Guella, F. Dini, F. Pietra, *Helv. Chim. Acta* **1996**, *79*, 2180–2189.

[6] G. Guella, F. Dini, F. Pietra, *Helv. Chim. Acta* **1996**, *79*, 439–448.

[7] a) G. Guella, invited lecture at "*III European Conference on Marine Natural Products*", Elmau Castle, Bavaria, Germany, September, **2002**; b) G. Guella, *"Marine Ciliates: an uncared Phylum"*, Symposium Lecture at CMIB, Naples, Italy, June, **2003**.

[8] G. Guella, F. Dini, F. Pietra, *Angew. Chem.* **1999**, *111*, 1217–1220; *Angew. Chem. Int. Ed.* **1999**, *38*, 1134–1136.

[9] R. A. Aungst, R. L. Funk, *J. Am. Chem. Soc.* **2001**, *123*, 9455–9456.

[10] a) G. Rosini, F. Laffi, E. Marotta, I. Pagani, P. Righi, *J. Org. Chem.* **1998**, *63*, 2389–2391; b) B. Snider, Q. Lu, *Synth. Commun.* **1997**, *27*, 1583–1600.

[11] K. C. Nicolaou, M. P. Jennings, P. Dagneau, *Chem. Commun.* **2002**, *21*, 2480–2481; K. C. Nicolaou, W. Tang, P. Dagneau, R. Faraoni, *Angew. Chem. Int. Ed.* **2005**, *44*, 3874–3879.

[12] R. W. Hoffmann, *Angew. Chem. Int. Ed.* **2000**, *39*, 2054–2070.

[13] *PCMOD 7.0*/*GMMX version 1.5, Serena Software*, P. O. Box 3076, Bloomington.

[14] M. J. Frisch, G. W. Trucks, H. B. Schlegel, G. E. Scuseria, M. A. Robb, J. R. Cheeseman, J. A. Montgomery Jr, T. Vreven, K. N. Kudin, J. C. Burant, J. M. Millam, S. S. Iyengar, J. Tomasi, V. Barone, B. Mennucci, M. Cossi, G. Scalmani, N. Rega, G. A. Petersson, H. Nakatsuji, M. Hada, M. Ehara, K. Toyota,

R. Fukuda, J. Hasegawa, M. Ishida, T. Nakajima, Y. Honda, O. Kitao, H. Nakai, M. Klene, X. Li, J. E. Knox, H. P. Hratchian, J. B. Cross, C. Adamo, J. Jaramillo, R. Gomperts, R. E. Stratmann, O. Yazyev, A. J. Austin, R. Cammi, C. Pomelli, J. W. Ochterski, P. Y. Ayala, K. Morokuma, G. A. Voth, P. Salvador, J. J. Dannenberg, V. G. Zakrzewski, S. Dapprich, A. D. Daniels, M. C. Strain, O. Farkas, D. K. Malick, A. D. Rabuck, K. Raghavachari, J. B. Foresman, J. V. Ortiz, Q. Cui, A. G. Baboul, S. Clifford, J. Cioslowski, B. B. Stefanov, G. Liu, A. Liashenko, P. Piskorz, I. Komaromi, R. L. Martin, D. J. Fox, T. Keith, M. A. Al-Laham, C. Y. Peng, A. Nanayakkara, M. Challacombe, P. M. W. Gill, B. Johnson, W. Chen, M. W. Wong, C. Gonzalez, J. A. Pople, *Gaussian 03, Revision C.02*, Gaussian, Inc., Wallingford, CT, **2004**.

[15] V. J. Paul, W. Fenical, *Tetrahedron* **1984**, *40*, 2913–2918.

[16] E. Fattorusso, S. Magno, E. Novellino, *Experientia* **1983**, *39*, 1275–1276.

[17] V. J. Paul, W. Fenical, *Phytochemistry* **1982**, *21*, 468–469.

[18] C. Lee, W. Yang, R. G. Parr, *Phys. Rev. B* **1988**, *37*, 785–789.

[19] a) A. D. Becke, *J. Chem. Phys.* **1993**, *98*, 5648–5652; b) B. Mielich, A. Savin, H. Stoll, H. Preuss, *Chem. Phys. Lett.* **1989**, *157*, 200–206.

[20] a) R. Krishnan, J. S. Binkley, R. Seeger, J. A. Pople, *J. Chem. Phys.* **1980**, *72*, 650–654; b) T. Clark, J. Chandrasekhar, G. W. Spitznagel, P. v. R. Schleyer, *J. Comput. Chem.* **1983**, *4*, 294–, 301; c) A. D. McLean, G. S. Chandler, *J. Chem. Phys.* **1980**, *72*, 5639–5648.

Received: May 21, 2007
Published Online: August 29, 2007

